

Genomic complexity predicts resistance to endocrine therapy and CDK4/6 inhibition in hormone receptor-positive (HR+)/HER2-negative metastatic breast cancer

A. A. Davis<sup>1</sup>, J. Luo<sup>2</sup>, T. Zheng<sup>3</sup>, C. Dai<sup>3</sup>, X. Dong<sup>3</sup>, L. Tan<sup>3</sup>, R. Suresh<sup>1</sup>, F. O. Ademuyiwa<sup>1</sup>, C. Rigden<sup>1</sup>, T. P. Rearden<sup>1</sup>, K. Clifton<sup>1</sup>, K. Weilbaecher<sup>1</sup>, A. Frith<sup>1</sup>, P. K. Tandra<sup>4</sup>, T. Summa<sup>1</sup>, B. Haas<sup>1</sup>, S. Thomas<sup>1</sup>, L. Hernandez-Aya<sup>1</sup>, L. L. Peterson<sup>1</sup>, X. Wang<sup>3</sup>, S. J. Luo<sup>3</sup>, K. Zhou<sup>3</sup>, P. Du<sup>3</sup>, S. Jia<sup>3</sup>, B. L. King<sup>3</sup>, J. Krishnamurthy<sup>4</sup>, C. X. Ma<sup>1</sup>

<sup>1</sup>Department of Medicine, Division of Oncology, Washington University School of Medicine in St. Louis, MO

<sup>2</sup>Division of Public Health Science, Department of Surgery, Biostatistics Shared Resource, Washington University in St. Louis, MO

<sup>3</sup>Predicine, Inc., Hayward, CA

<sup>4</sup>Division of Oncology/Hematology, University of Nebraska Medical Center, Omaha, NE.

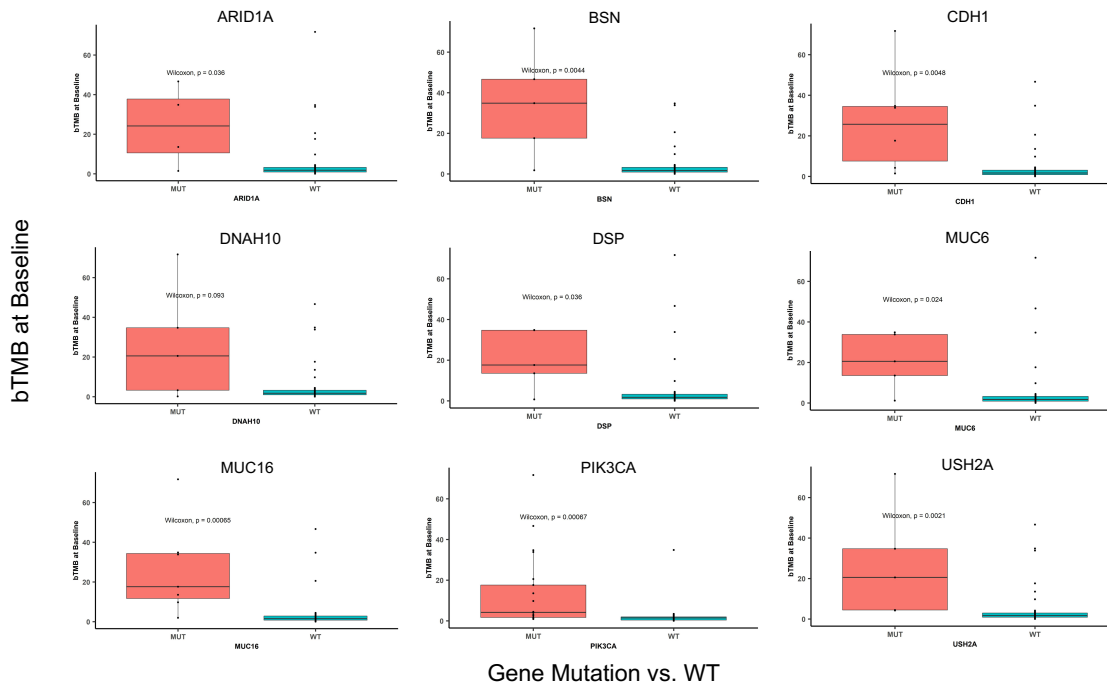
Corresponding authors:

**\*Corresponding author**, Dr. Andrew A. Davis, Section of Medical Oncology, Division of Oncology, Department of Medicine, Siteman Cancer Center, Washington University School of Medicine, 660 South Euclid Avenue, St Louis, MO 63110, USA. Tel: 314-273-3581; Email: [aadavis@wustl.edu](mailto:aadavis@wustl.edu)

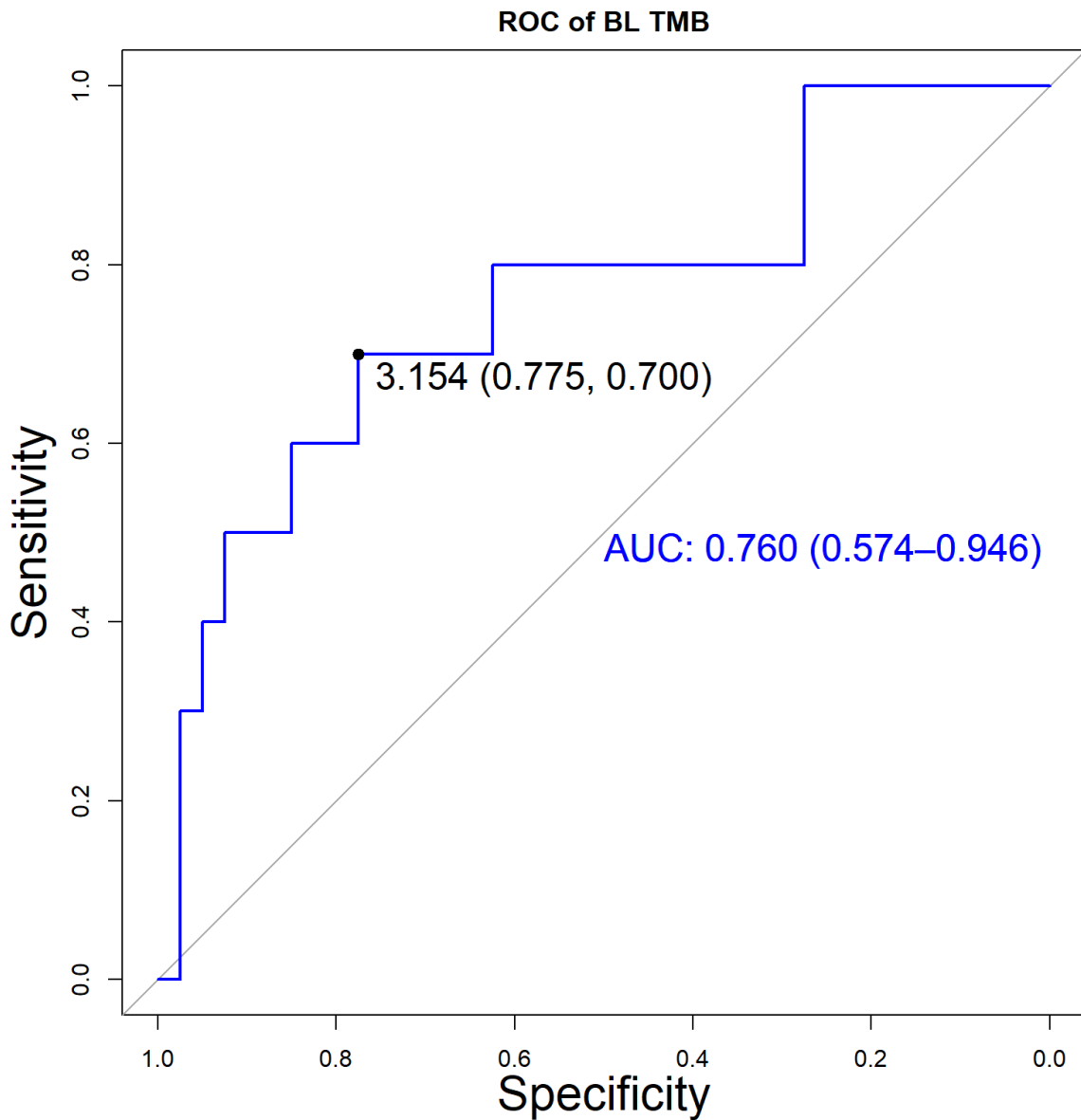
**\*Corresponding author**, Dr. Cynthia X. Ma, Section of Medical Oncology, Division of Oncology, Department of Medicine, Siteman Cancer Center, Washington University School of Medicine, 660 South Euclid Avenue, St Louis, MO 63110, USA. Tel: 314-362-9383, Fax: 314-362-7086. Email: [cynthiama@wustl.edu](mailto:cynthiama@wustl.edu); Orcid ID: <https://orcid.org/0000-0002-8156-7492>

## SUPPLEMENTARY FIGURES

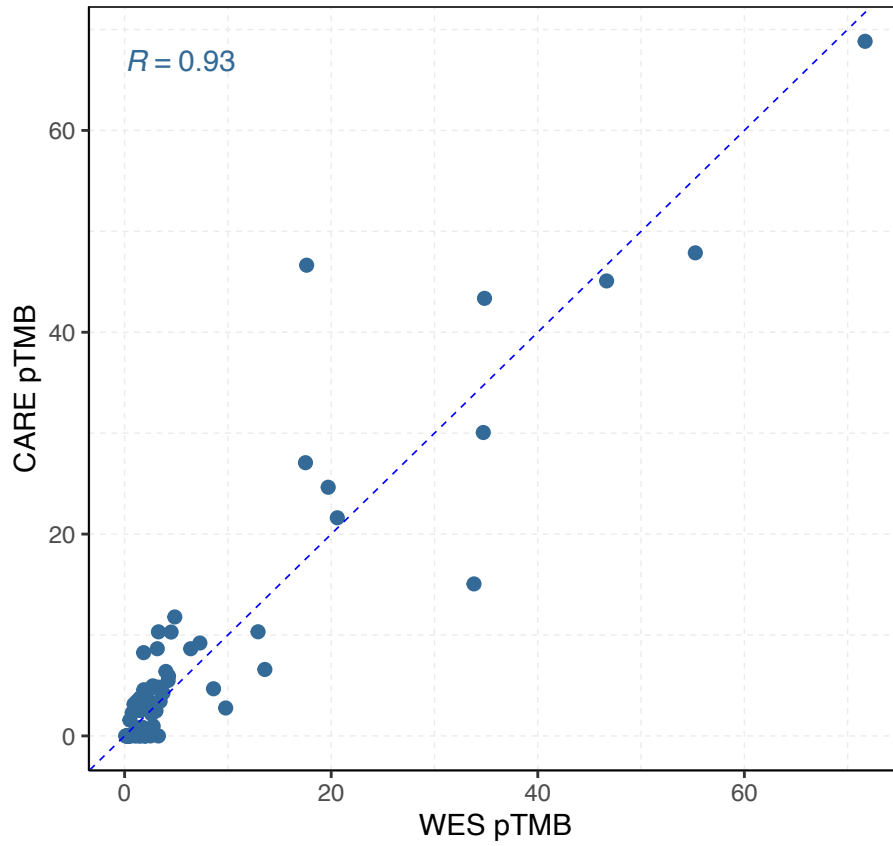
| TABLE OF CONTENTS   | Page |
|---|------|
| <b>Figure S1. High bTMB is associated with the presence of specific mutations.</b>  | 3    |
| <b>Figure S2. ROC analysis to determine optimal bTMB cutoff.</b>  | 4    |
| <b>Figure S3. High correlation between bTMB determined from WES and a 152-gene targeted sequencing panel.</b>                   | 5    |
| <b>Figure S4. Association between high cfDNA yield and shorter PFS.</b>   | 6    |
| <b>Figure S5. High baseline tumor fraction is associated with shorter PFS.</b>  | 7    |
| <b>Figure S6. bTMB scores are not associated with sites of metastatic spread.</b>   | 8    |
| <b>Figure S7. Specific oncogenic signaling pathways are more frequently altered in patients with high bTMB and bCNB scores.</b> | 9    |
| <b>Figure S8. Genomic landscape of all patients at baseline.</b>  | 10   |
| <b>Figure S9. bTMB and bCNB at baseline vs. progression.</b>  | 11   |
| <b>Figure S10. Correlation between baseline bCNB and bTMB.</b>  | 12   |
| <b>Figure S11. Comparison of ctDNA dynamics as measured by ctDNA fraction and bCNB during treatment and progression.</b>        | 13   |
| <b>Figure S12. Genome-wide plots of copy number changes across treatment time points.</b>                                       | 14   |
| <b>Figure S13. Copy number changes detected for RB1 and BRCA2 genes across treatment time points.</b>                           | 15   |
| <b>Figure S14. Relationship between ctDNA fraction and bTMB and bCNB</b>  | 16   |
| <b>Figure S15. Relationship between tumor fraction and bCNB.</b>  | 17   |



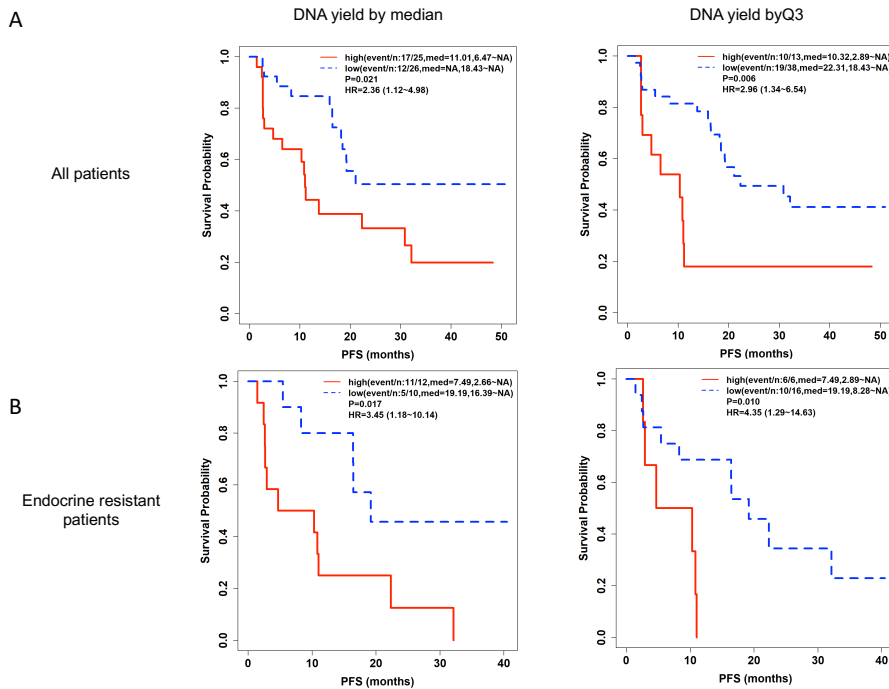
**Supplementary Figure 1. High bTMB is associated with the presence of specific gene alterations.** High baseline bTMB scores were significantly associated with higher frequencies of mutations in *ARID1A* ( $P = 0.036$ ), *BSN* ( $P = 0.004$ ), *CDH1* ( $P = 0.005$ ), *DNAH10* ( $P = 0.093$ ), *DSP* ( $P = 0.036$ ), *MUC6* ( $P = 0.024$ ), *MUC16* ( $P = 0.0007$ ), *PIK3CA* ( $P = 0.0007$ ) AND *USH2A* ( $P = 0.002$ ) (Wilcoxon test). Following adjustment for FDR, associations remained significant for *PIK3CA* ( $P = 0.016$ ), *CDH1* ( $P = 0.036$ ) and *USH2A* ( $P = 0.032$ ).



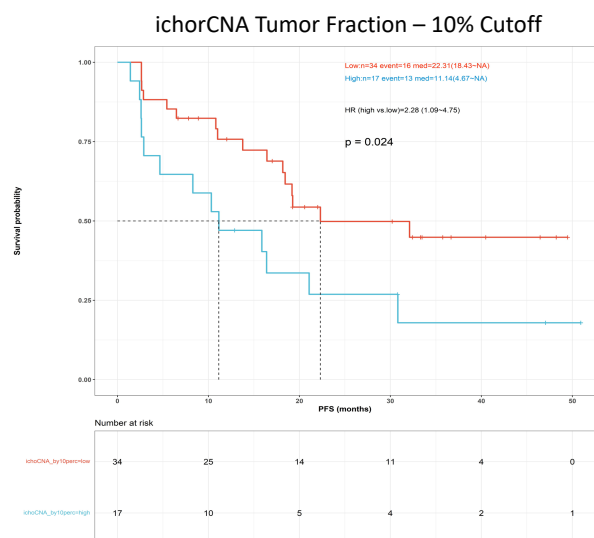
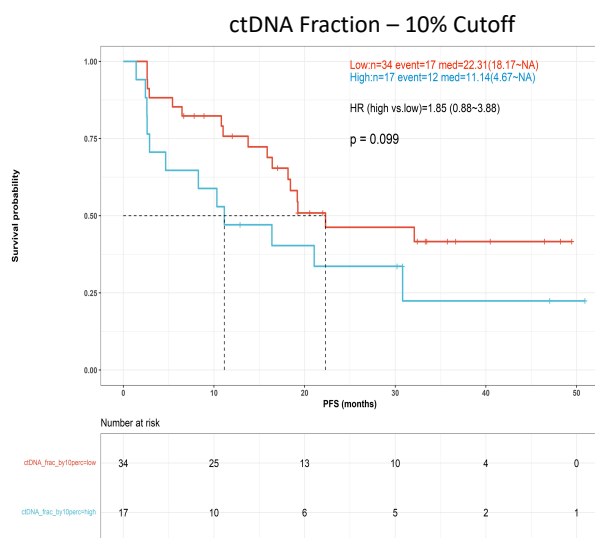
**Supplementary Figure 2. ROC analysis to determine optimal cutoff point of bTMB for clinical benefit.** To gauge the predictive ability of baseline bTMB (N = 50) and to identify an optimal cutoff point for clinical benefit (CB), we conducted ROC analysis on baseline bTMB with CB. The ROC curve was plotted for each potential cutoff on the bTMB score, with estimated AUC (0.76, 95% CI=0.574~0.946) and the optimal cutoff point identified at 3.154 with the corresponding specificity (0.775) and sensitivity (0.7). The optimal cutoff point of 3.154 coincides with the upper 75% quartile (3.8) of patients' bTMB, which was used to dichotomize patients throughout this study, unless otherwise stated.



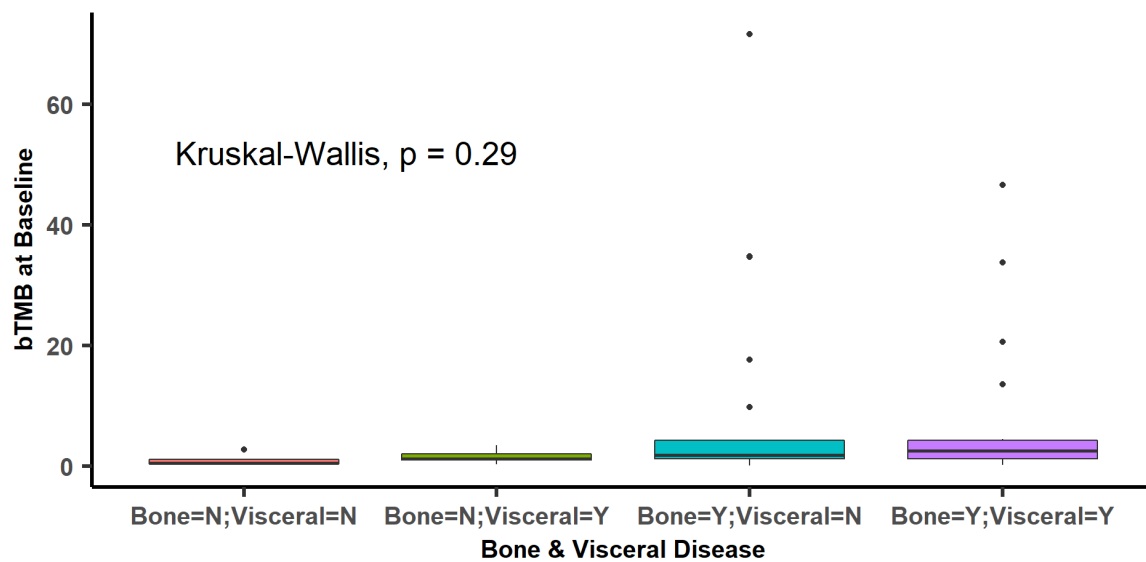
**Supplementary Figure 3. High correlation between bTMB determined from WES and a 152-gene targeted sequencing panel.** bTMB levels generated from 50 baseline samples using the PredicineWES™ and PredicineCARE™ sequencing assays were highly correlated ( $R = 0.93$ , Spearman's Rank Test).



**Supplementary Figure 4. High baseline cfDNA yield is associated with shorter PFS.** A) High cfDNA yield in plasma samples collected from 51 patients at baseline was significantly associated with shorter PFS compared to patients with lower cfDNA yield, as defined by median ( $P = 0.021$ ) and upper quartile ( $P = 0.006$ ) cutoffs (log rank test). B) High cfDNA yield in plasma samples collected from 22 patients with endocrine resistance was significantly associated with shorter PFS, as defined by median ( $P = 0.017$ ) and upper ( $P = 0.01$ ) quartile cutoffs (log rank test).

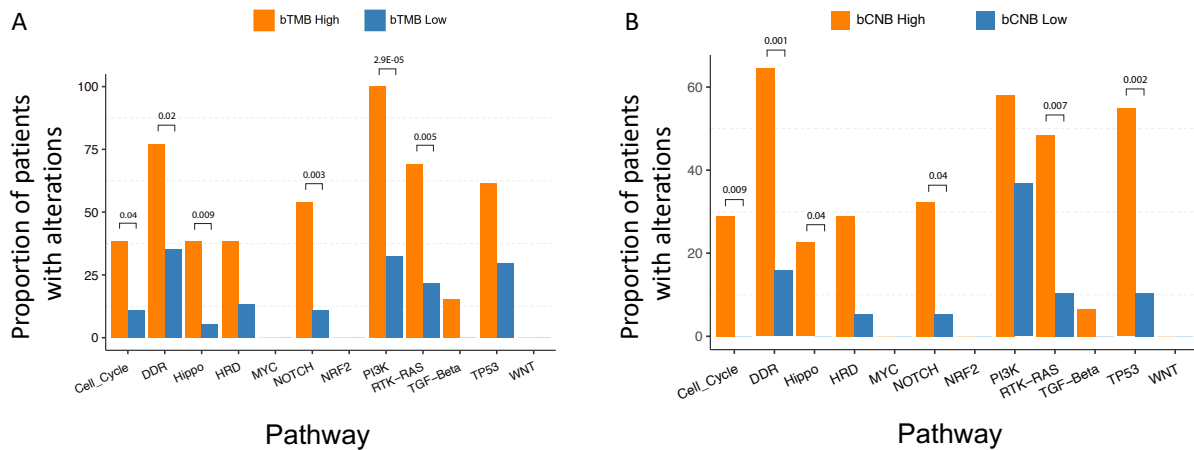


**Supplementary Figure 5. High baseline tumor fraction is associated with shorter PFS.** PFS was analyzed in association with ctDNA fraction and tumor fraction (TF) levels determined for 51 baseline samples. A 10% cutoff level was used to dichotomize patients for Kaplan-Meier survival analysis. A) High ctDNA fraction based on mutational analysis was not significantly associated with shorter PFS. B) Patients with high ichorCNA-inferred tumor fraction had significantly shorter PFS compared to patients with low TF (P = 0.024, log rank test).

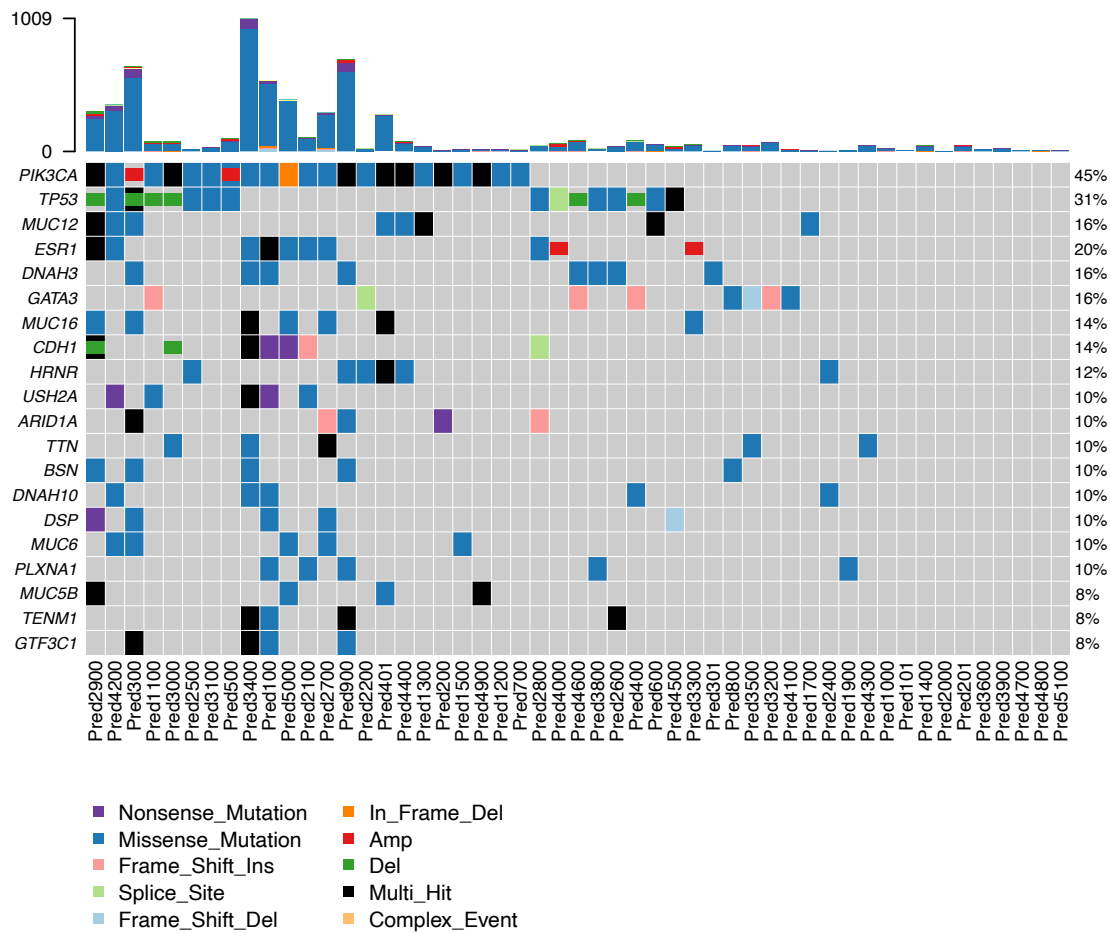


**Supplementary Figure 6. bTMB scores are not associated with sites of metastatic spread.** bTMB scores across 50 patients at baseline are not significantly different across patients with vs. without bone and/or visceral disease (Kruskal-Wallis test).

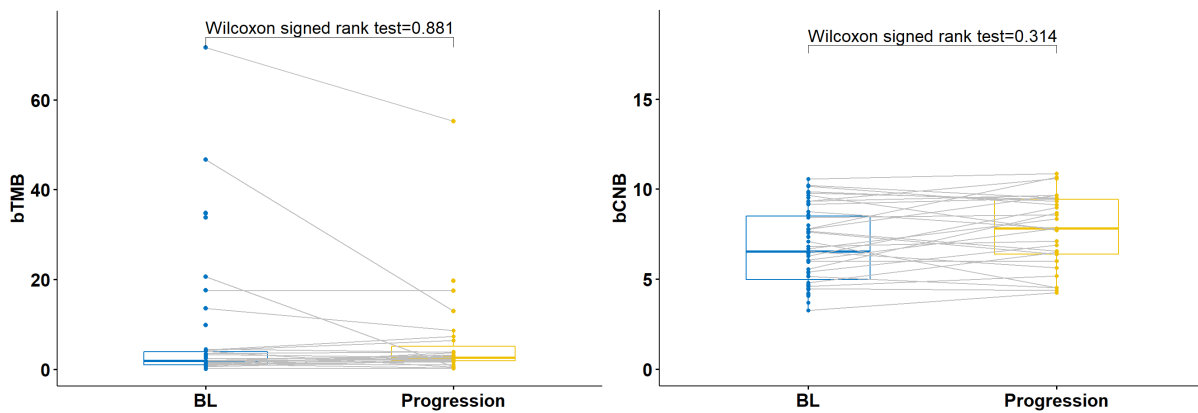




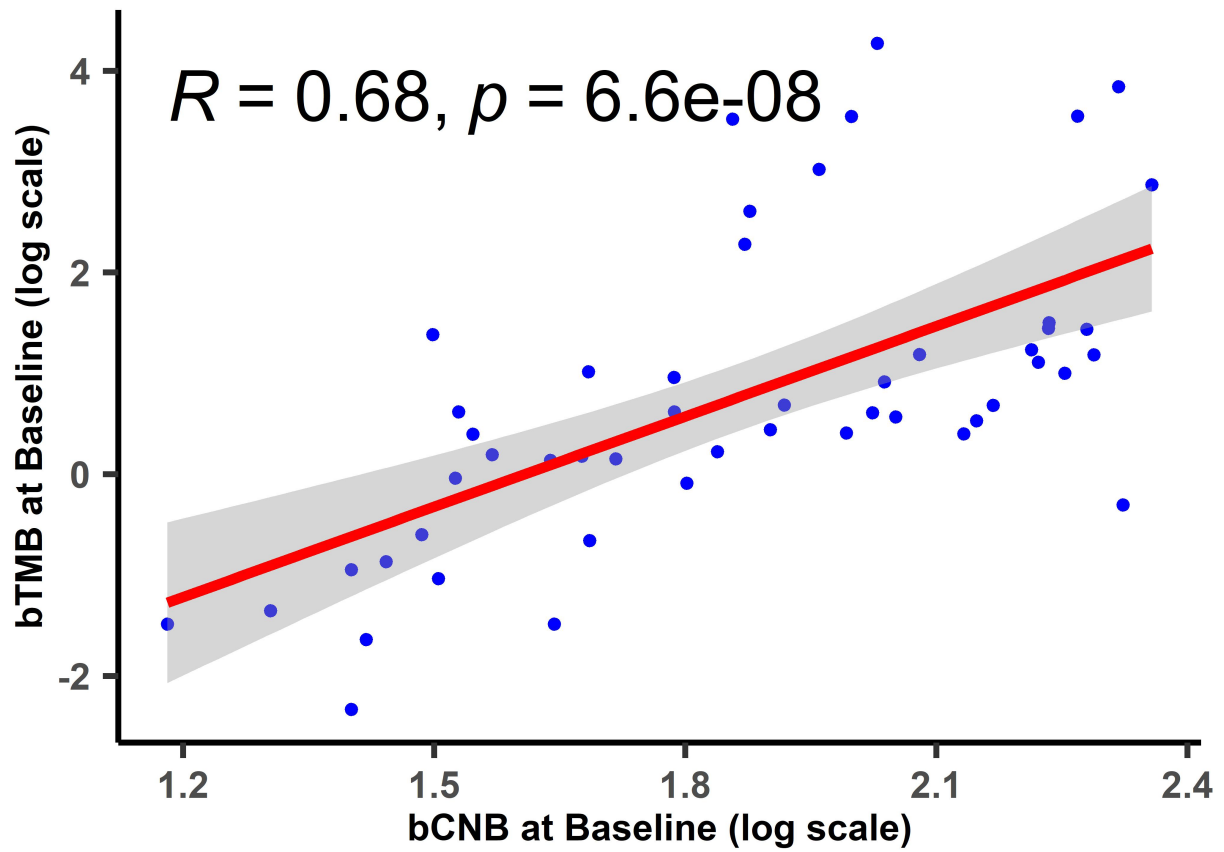
**Supplementary Figure 7. Specific oncogenic signaling pathways are more frequently altered in patients with high bTMB and bCNB scores.** A) Significantly higher frequencies of alterations were observed in high (N = 13) vs. low (N = 37) bTMB patients across breast cancer driver genes in the Cell Cycle, DNA Damage Repair (DDR), Hippo, Notch, PI3K and Receptor Tyrosine Kinase (RTK-RAS), Hippo and PI3K oncogenic signaling pathways (Fisher's Exact Test). Following adjustment for FDR, associations remained significant for the Notch (P = 0.03), PI3K (P =  $2.6 \times 10^{-4}$ ) and Receptor Tyrosine Kinase (RTK)-RAS (P = 0.03) pathways. B) Significantly higher frequencies of alterations were also observed in high vs. low bCNB patients across breast cancer driver genes in the Cell Cycle, DDR, Hippo, Notch, RTK-RAS and TP53 oncogenic signaling pathways (Fisher's Exact Test). Following adjustment for FDR, associations remained significant for the DDR (P = 0.01), RTK-RAS (P = 0.05) and TP53 (P = 0.02) pathways.



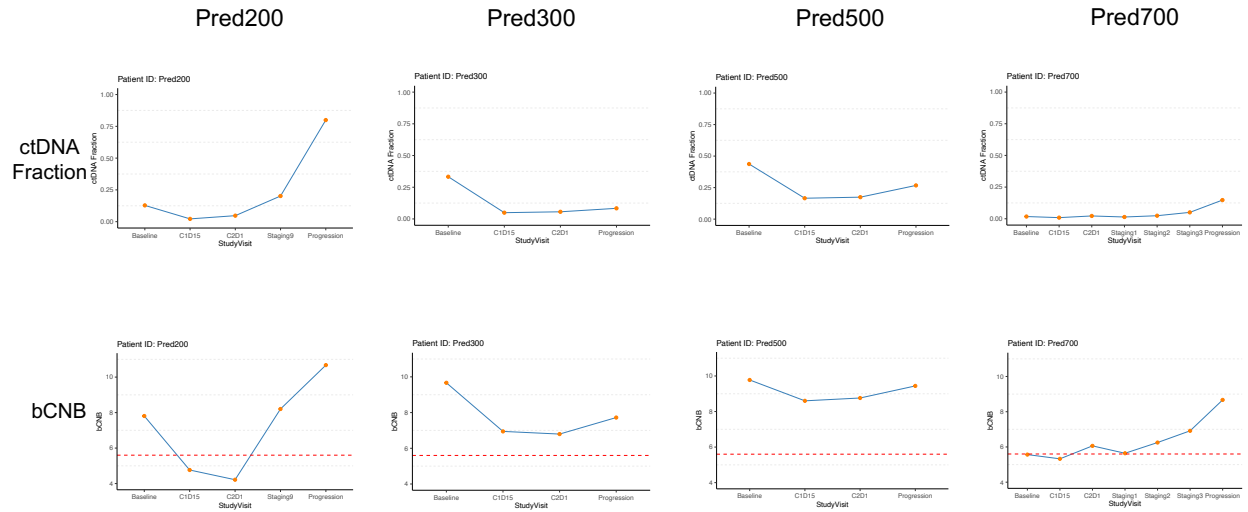
**Supplementary Figure 8. Oncoprint showing landscape of genomic alterations across all patients at baseline.** Frequencies of alterations across all 51 patients, including SNVs and CNVs across all patients are shown on the right. The bars on top of each column represent the total number of alterations detected in a given patient.



**Supplementary Figure 9. bTMB and bCNB at baseline vs. progression timepoints.** No significant differences were observed in median bTMB or bCNB levels detected in baseline (N = 50) vs. progression samples (N = 28) (Wilcoxon signed rank test).

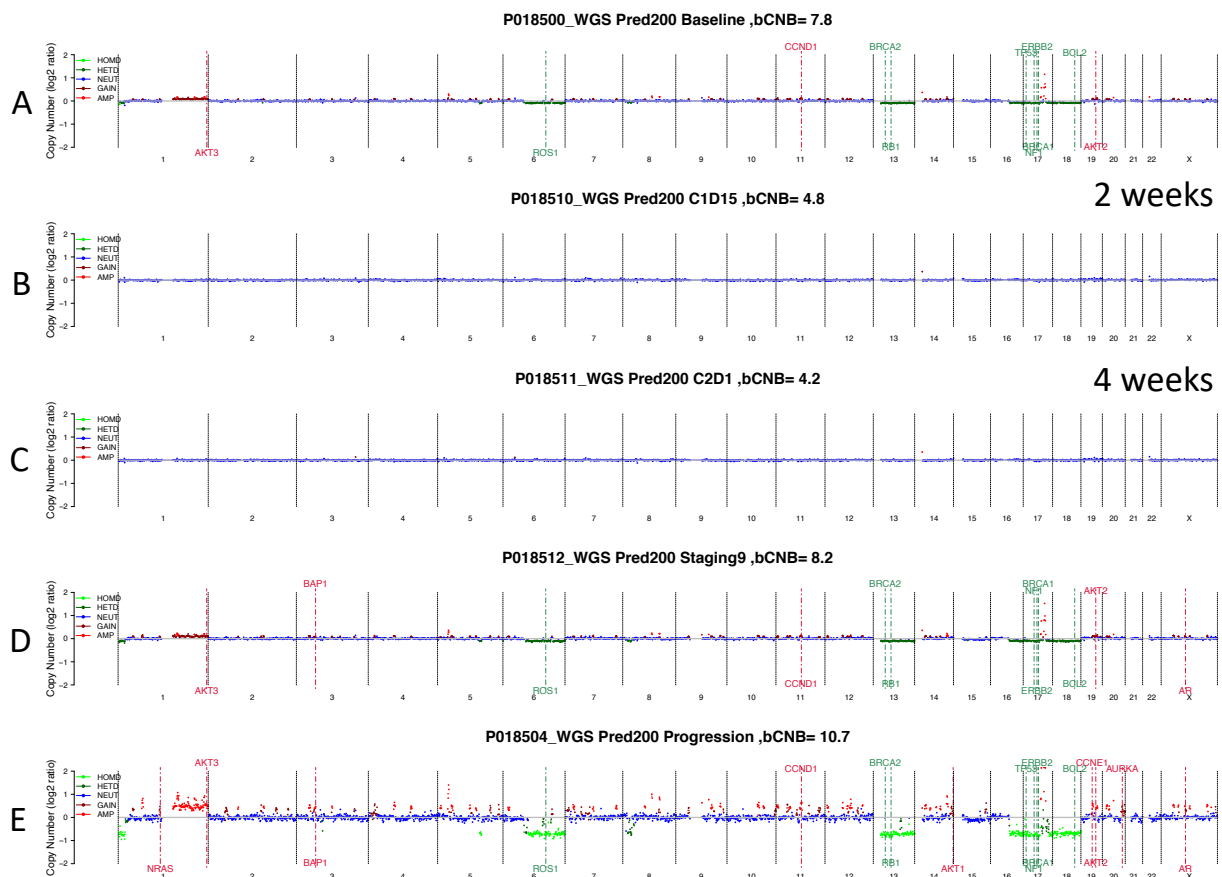


**Supplementary Figure 10. Correlation between baseline bTMB and bCNB scores.** bTMB and bCNB scores across 50 patients at baseline were correlated ( $R = 0.68$ , Spearman's Rank Correlation Coefficient).

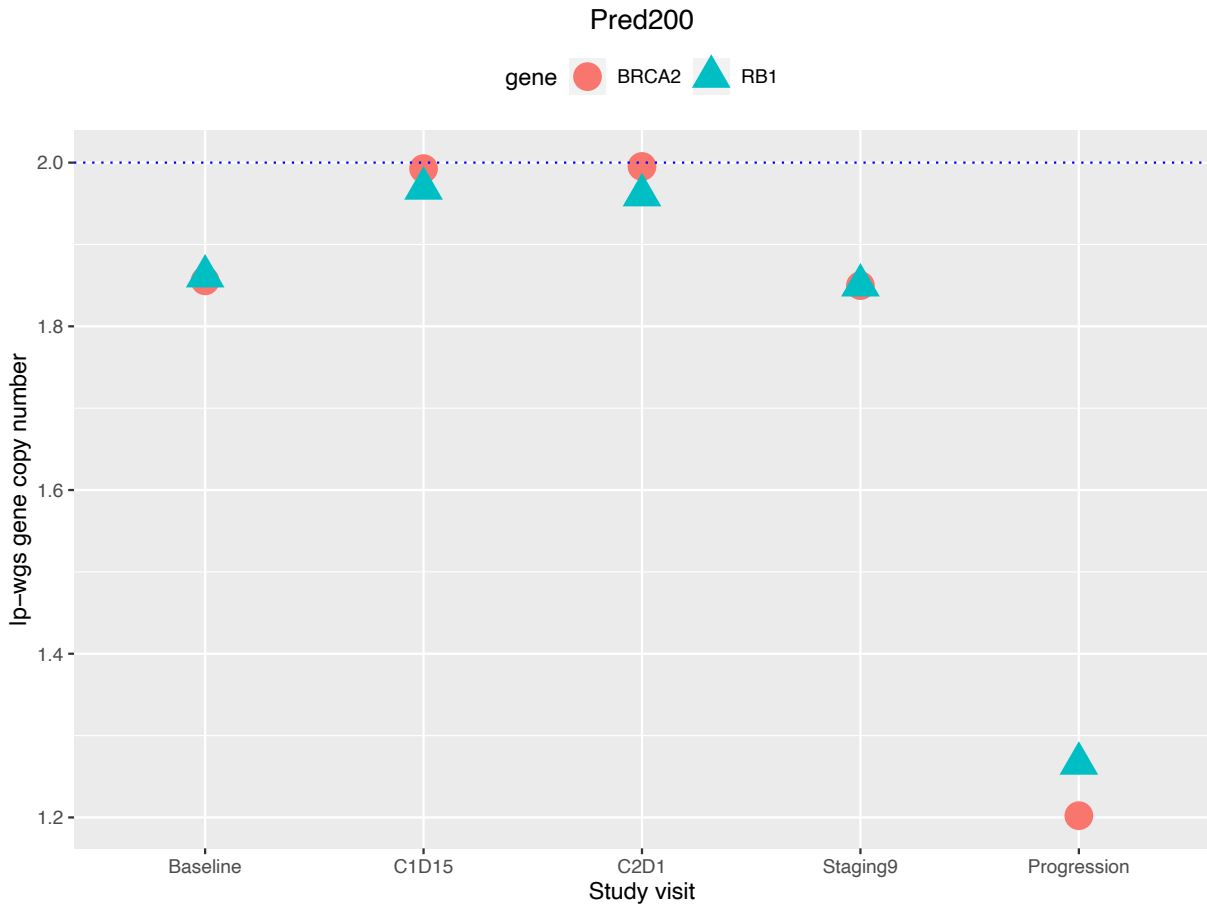


Study Visit: Baseline > C1D15 > C2D1 > Staging > Progression

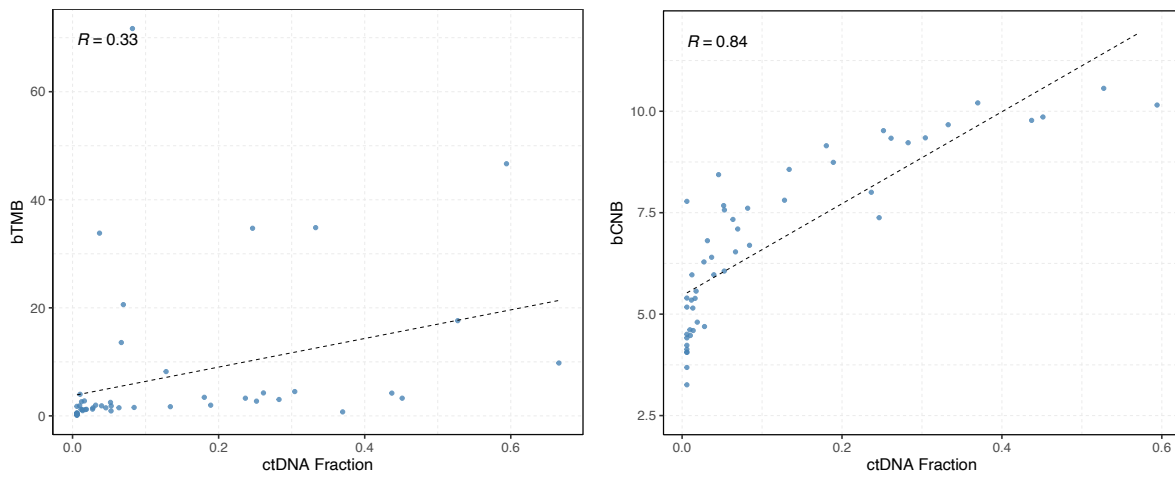
**Supplementary Figure 11. Comparison of ctDNA dynamics as measured by ctDNA fraction and bCNB during treatment and progression.** Serial blood samples from 4 patients (Pred200, Pred300, Pred500 and Pred700) were analyzed by PredicineATLAS™ to derive ctDNA fraction values and by PredicineCNB™ to derive bCNB scores at baseline, C1D15, D2D1, staging and progression timepoints. Similar dynamics are observed using both NGS metrics. Pearson correlations between matched longitudinal profiles of ctDNA fraction and bCNB were 0.86, 0.99, 0.92, 0.98 (average = 0.94) for patients Pred200, Pred300, Pred500 and Pred700, respectively.



**Supplementary Figure 12. Genome-wide plots of copy number changes across treatment time points.** Copy number changes observed at baseline, C1D15, C2D1, staging visit 9 and progression time points for patient Pred200 (from **Supplementary Figure 11**), revealing dramatic changes in copy number variation status over the course of treatment, even at time points occurring just 2 and 4 weeks after treatment initiation.

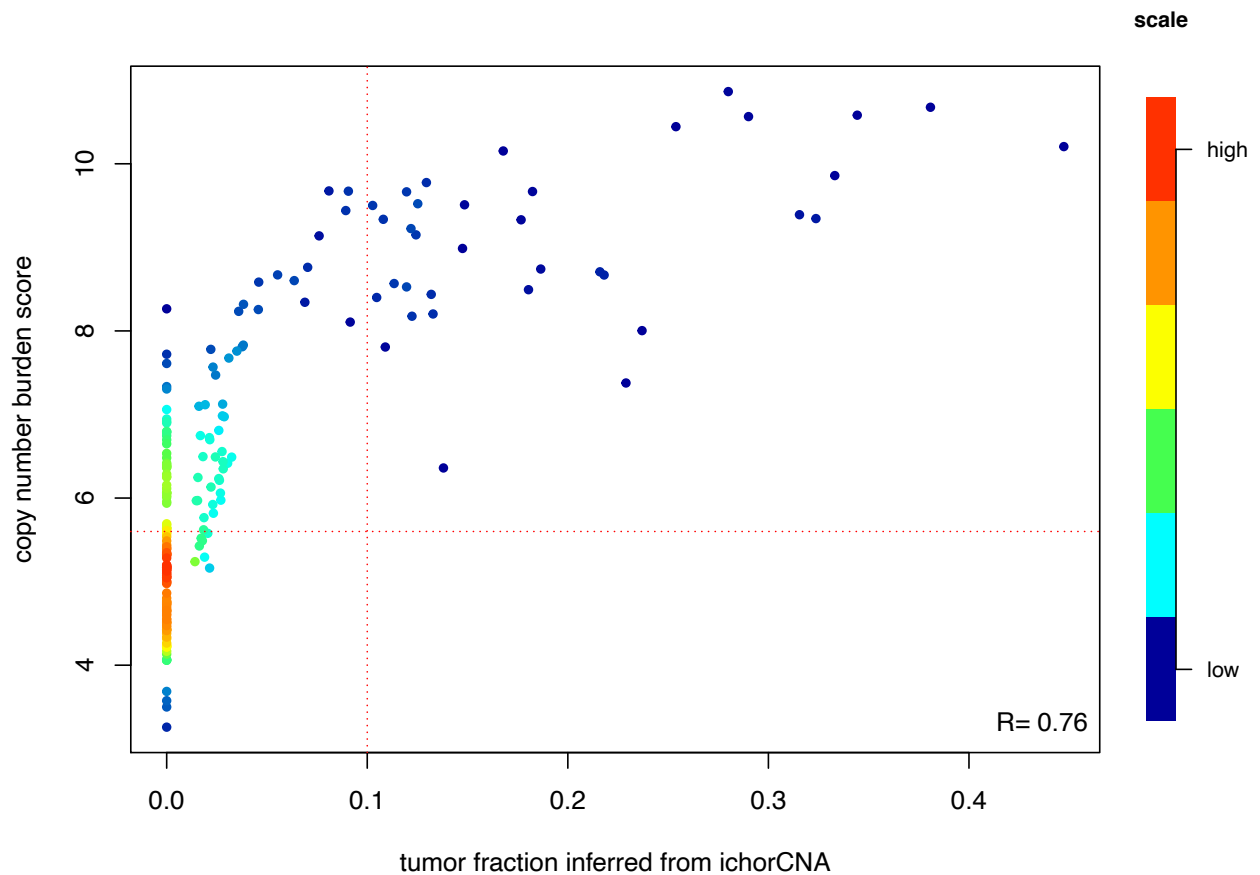


**Supplementary Figure 13. Copy number changes detected for RB1 and BRCA2 genes across treatment time points.** Copy number changes detected by LP-WGS are shown at baseline and across treatment time points (b C1D15, C2D1, staging visit 9 and progression) for patient Pred200 (from **Supplementary Figure 11**). While significant copy number variation for RB1 and BRCA2 is not detected at time points C1D15 and C2D1 (in keeping with low bCNB scores), copy number variation is detected at both genes at the other time points (when bCNB is high), particularly at the time of progression.



**Supplementary Figure 14. Relationship between ctDNA fraction and bTMB and bCNB.** Scatter plots of bTMB vs. ctDNA fraction (left) and bCNB vs. ctDNA fraction (right) based on 51 baseline samples. While no correlation is observed between ctDNA fraction and bTMB scores, a strong correlation is observed between ctDNA fraction and bCNB scores ( $R = 0.84$ , Pearson's correlation coefficient).





**Supplementary Figure 15. Relationship between tumor fraction and bCNB.** Scatter plots of bCNB scores in association with ichorCNA-derived TF levels in 216 samples collected over multiple treatment time points. bCNB scores were strongly associated with TF levels ( $R = 0.76$ , Pearson's correlation coefficient) with the association being strongest at higher TF levels. This plot illustrates the high sensitivity of bCNB to detect tumor-associated copy number variation in plasma samples with low (<5%) tumor fraction. The color scale emphasizes the density of data points in a given region of the plot.